

# Field-effect control of protein transport in a nanofluidic transistor circuit

Cite as: Appl. Phys. Lett. **88**, 123114 (2006); <https://doi.org/10.1063/1.2186967>

Submitted: 29 September 2005 • Accepted: 31 January 2006 • Published Online: 24 March 2006

Rohit Karnik, Kenneth Castellino and Arun Majumdar



View Online



Export Citation

## ARTICLES YOU MAY BE INTERESTED IN

[Review article: Fabrication of nanofluidic devices](#)

Biomicrofluidics **7**, 026501 (2013); <https://doi.org/10.1063/1.4794973>

[Solid-state nanopore hydrodynamics and transport](#)

Biomicrofluidics **13**, 011301 (2019); <https://doi.org/10.1063/1.5083913>

[Ion transport through nanoslits dominated by the effective surface charge](#)

Applied Physics Letters **86**, 253111 (2005); <https://doi.org/10.1063/1.1954899>



**Characterizing nanostructures?**  
Learn about a new way to get high-quality data in a fraction of the time

Read the tech note

Lake Shore  
CRYOTRONICS

# Field-effect control of protein transport in a nanofluidic transistor circuit

Rohit Karnik and Kenneth Castellino

*Department of Mechanical Engineering, University of California, Berkeley, California 94720*

Arun Majumdar<sup>a)</sup>

*Department of Mechanical Engineering, University of California, Berkeley, California 94720*

*and Materials Sciences Division, Lawrence Berkeley National Laboratory, Berkeley, California 94720*

(Received 29 September 2005; accepted 31 January 2006; published online 24 March 2006)

Electrostatic interactions play an important role in nanofluidic channels when the channel size is comparable to the Debye screening length. Electrostatic fields have been used to control concentration and transport of ions in nanofluidic transistors. Here, we report a transistor-reservoir-transistor circuit that can be used to turn “on” or “off” protein transport using electrostatic fields with gate voltages of  $\pm 1$  V. Our results suggest that global electrostatic interactions of the protein were dominant over other interactions in the nanofluidic transistor. The fabrication technique also demonstrates the feasibility of nanofluidic integrated circuits for the manipulation of biomolecules in picoliter volumes. © 2006 American Institute of Physics.

[DOI: 10.1063/1.2186967]

Analysis of biological samples and chemical species is central to clinical diagnostics, gene sequencing, drug discovery, and pharmaceuticals. Such analysis requires a series of steps such as separation, purification, concentration enhancement, detection, and activity assays. Microfluidics has been an area of intense research, where miniaturization promises faster analysis with very low sample consumption and ultimately “lab-on-a-chip” systems.<sup>1</sup> Scaling of certain physical phenomena can be exploited by miniaturization,<sup>2</sup> as exemplified in capillary electrophoresis, droplet-based systems, electroosmotic pumping, etc. However, if the dimensions of fluidic channels are further decreased to the nanoscale (below  $\sim 100$  nm), they become comparable to a length scale that characterizes the range of electrostatic interactions. This length, known as the Debye length, increases with decreasing ionic concentration and is typically 1–100 nm in aqueous solutions.<sup>3</sup> In such nanofluidic channels, surface charge causes the concentration of co-ions to decrease and that of counterions to increase to neutralize the surface charge. Thus, charge plays a critical role, and phenomena such as surface charge-governed transport,<sup>4–6</sup> concentration enhancement and depletion,<sup>7</sup> and biosensing<sup>8</sup> were reported.

Recently, we demonstrated electrostatic control of ions and DNA molecules in a nanofluidic transistor,<sup>6,9,10</sup> which is a nanofluidic channel with a gate electrode that enables field-effect control of charged species [Fig. 1(a)]. However, field-effect control of proteins is more involved due to their complex nature. Proteins are highly surface active and they interact with solid-liquid interfaces primarily through three subprocesses:<sup>11</sup> (1) structural rearrangements in the protein molecule, (2) dehydration of parts of protein and surface (hydrophobic effect), and (3) redistribution of charged groups in the interfacial layer. Global electrostatic effects may dominate when the protein is structurally stable and the solid surface is hydrophilic.<sup>11</sup> For electrostatic field effect to dominate, it is essential that the native nanochannel surface is electrically neutral. The ideal system for field-effect con-

trol is, therefore, that of a hydrophilic, neutral surface, and a charged, stable protein. The current work demonstrates flow control of the protein avidin, which is enabled by two major modifications of our original work: (a) fabrication of a transistor-reservoir-transistor circuit, which allowed for the examination of protein flow via filling or emptying of the reservoir, and (b) chemical modification of the native silica surface.

The transistor-reservoir-transistor circuit [Figs. 1(b) and 1(c)] was fabricated using sacrificial polycrystalline silicon,

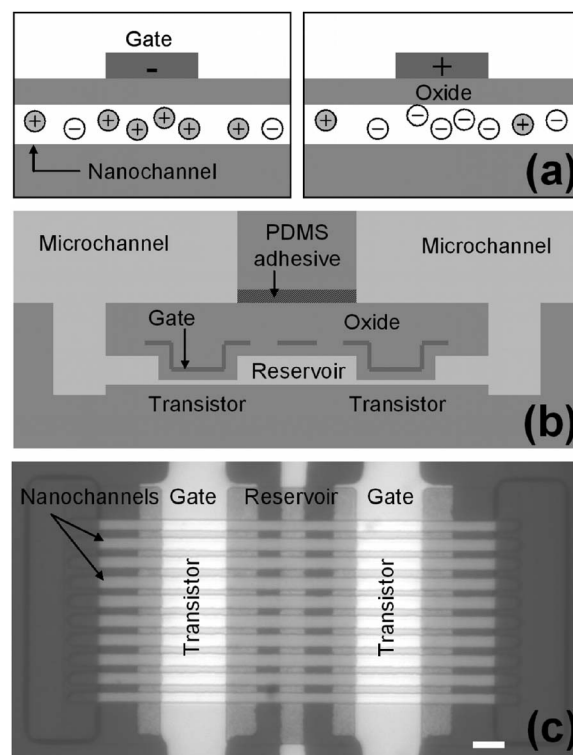


FIG. 1. Nanofluidic transistor. (a) Schematic of a nanofluidic transistor. The gate voltage can be used to control the ionic concentration in the nanochannel via field effect. (b) Schematic of the transistor-reservoir-transistor system connected with microfluidic channels on either side. (c) Micrograph of the fabricated device, with 120  $\mu\text{m}$  long channels (scale bar is 10  $\mu\text{m}$ ).

<sup>a)</sup> Author to whom correspondence should be addressed; electronic mail: majumdar@me.berkeley.edu

as described in our previous report.<sup>6</sup> A device consisted of ten 120  $\mu\text{m}$  long parallel channels and was designed in a way that fluorescence signals could be observed in each channel simultaneously. Two polycrystalline silicon deposition steps allowed for the variation of nanochannel height between 30 and 330 nm; the 30 nm channels formed the nanofluidic transistors while the 330 nm channels formed the reservoirs. Two chromium gate electrodes were patterned perpendicular to the two 30 nm channels, and were separated by a 130 nm gate oxide to form two nanofluidic transistors. In addition, a central electrode was patterned over the 330 nm reservoir in order to block off stray light or interference from the polydimethylsiloxane (PDMS) used for bonding.<sup>12</sup> The reservoir also yields a higher fluorescence signal due to a longer optical path resulting from its greater height. The two gate electrodes over the 30 nm channels were designed to overlap with the 330 nm sections to ensure that the entire 30 nm channel region was gated. Ag/AgCl electrodes were used to make electrical connections with the solutions in each microchannel, while contact pads were provided for each gate electrode. The control voltages were applied using a DAQ card (National Instruments NI-6229) controlled by Matlab. During the course of the experiments, the gate electrodes over the reservoir and the transistor on the right were grounded. Since silica has a negative charge in the range of 2–100  $\text{mC}/\text{m}^2$ ,<sup>4,6</sup> the native silica surface of the nanochannels was modified by treating it with a 2% solution of 3-glycidioxypropyl trimethoxysilane (Gelest Inc.) in ethanol for 1 h followed by 50 mM ethanolamine (Sigma-Aldrich) in de-ionized water for 30 min. We found the resulting surface to be highly hydrophilic with a surface charge (measured using conductance of uniform 30 nm nanochannels)<sup>8</sup> less than 0.2  $\text{mC}/\text{m}^2$ . The protein used in the experiments, avidin, is a positively charged globular protein with a pI of 10.5 and is structurally highly stable.<sup>13</sup> Therefore, the system used consisted of a nearly electrically neutral hydrophilic surface and a charged, stable, globular protein.

For the experiments, the nanochannel surfaces were first modified as described above. The microchannel on the left (see Fig. 1) was filled with a solution of  $\sim 30 \mu\text{M}$  avidin labeled with Alexa 488 (Molecular Probes) in 10  $\mu\text{M}$  KCl solution and the microchannel on the right was filled with a 10  $\mu\text{M}$  KCl solution. The Debye length ranges from approximately 30 to 100 nm for 100–10  $\mu\text{M}$  KCl solutions. With the left gate voltage at 0.5 V, a fluorescence signal was observed in the left reservoir, but no significant fluorescence was observed in the channel or in the central reservoir, consistent with the fact that positively charged avidin was repelled out of the channel. When the left gate was switched to  $-1$  V, a fluorescent front was seen to progress from the reservoir into the 30 nm channel [Fig. 2]. Because avidin is positively charged, the concentration is expected to be enhanced on the application of a negative gate voltage. This front eventually reached the central reservoir and started filling it [Fig. 2]. This process is slow, because it is driven by diffusion alone and required about 30 min to reach the reservoir. Diffusivity ( $D$ ) of avidin may be approximately estimated by  $D \sim l^2/t = (20 \mu\text{m})^2/(10 \text{ min}) = 7 \times 10^{-13} \text{ m}^2/\text{s}$ . This value is about two orders of magnitude smaller than typical protein diffusivities in dilute solutions, which suggests that interactions within the channels dramatically decreased the diffusivity of avidin. When the gate voltage was

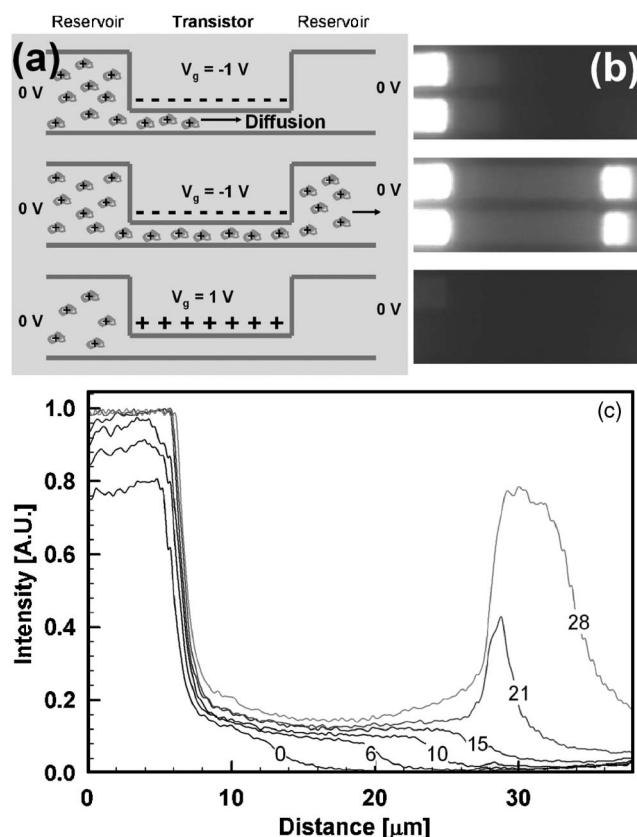


FIG. 2. Effect of gate voltage without bias between the microchannels. (a) Schematic showing diffusion of avidin when the transistor is turned on without bias between the microchannels. (b) Fluorescence images corresponding to (a). (c) Line plots of fluorescence intensities (background subtracted) along a representative channel showing diffusion of avidin along the channel. Numbers on the line plots denote time in minutes.

changed from  $-1$  to  $+1$  V, the fluorescence intensity decreased, indicating that the avidin had been repelled out of the gated region [Fig. 2]. Figure 2(c) shows the fluorescence intensity along a representative channel showing the fluorescent front in the 30 nm channel and the filling of the reservoir.

To examine the transport under bias, the microchannel on the right was held at  $-1$  V, while the gate voltage of the transistor on the left was switched between  $-1$  and  $+1$  V. The gate voltage of the transistor on the right was maintained at  $0$  V and we expect the protein to flow into the central reservoir through the transistor on the left and flow out through the transistor on the right. The fluorescence intensity in the central reservoir was observed to increase when the transistor was “on” ( $-1$  V) and to decrease when the transistor was switched “off” ( $1$  V) [Fig. 3(a)]. The filling and emptying of the central reservoir is seen clearly in the line plots across the central reservoir [Fig. 3(b)]. With the application of a negative gate voltage to the transistor on the left (on state), the influx of protein into the central reservoir is expected to increase. With a positive gate bias (off state), the influx should decrease, leading to depletion of protein because of outflow through the transistor on the right. This result demonstrates field-effect control of protein transport in nanofluidic transistors.

The current devices were found to fail at gate voltages of approximately 2 V by electrical breakdown at the steps where the nanochannel widened from 30 to 330 nm. In addition, they exhibited gate leakage. This defect was possibly

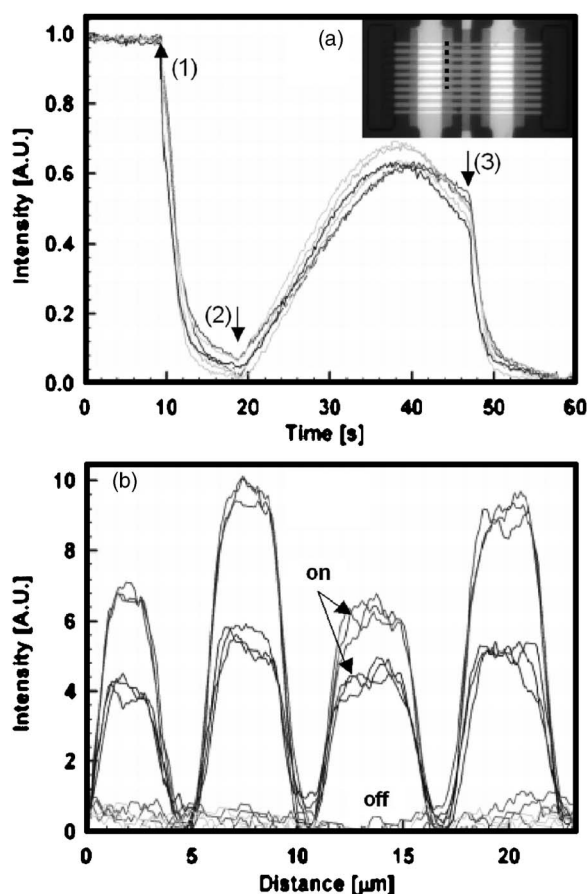


FIG. 3. Effect of gate voltage with bias applied between the microchannels. (a) Variation of fluorescence intensity in the central reservoirs (measured along the dotted line, inset) with time as the transistor is switched on and off. Gate voltage is switched from  $-1$  V (on) to  $1$  V (off) at (1), to  $-1$  V (on) at (2) and to  $1$  V (off) at (3). (b) Line plots of fluorescence intensity (background subtracted) in the central reservoirs (along dotted line, inset) show the transistor in the on and off states corresponding to the sequence in (a).

due to inadequate step coverage by the dielectric oxide or due to breakdown caused by sharp edges at the step. While the limited voltage range of operation precluded a detailed characterization of the transistor-reservoir-transistor circuit,

field-effect control of avidin is clearly evident from the above experiments. Our results suggest that global electrostatic interaction was the dominant interaction of avidin within the nanochannels. Fabrication of the transistor-reservoir-transistor circuit using standard lithography demonstrates the feasibility of integration into networks or nanofluidic circuits. Manipulation of biomolecules in such nanofluidic circuits could lead to new types of separation, flow control, and concentration enhancement techniques based on the flexibility of field-effect control in nanofluidic transistors. Liquid volumes in our experiments were less than  $1$   $\mu\text{l}$ , which suggests that it may be possible to use nanofluidic integrated circuits to study the contents of a single biological cell.

The authors thank Peidong Yang and Rong Fan (University of California at Berkeley and Lawrence Berkeley National Laboratory) as well as Henry Lin, Ram Datar, and Richard Cote (USC) for their continued collaboration in nanofluidics research. This work was supported in part by the following: Basic Energy Sciences, Department of Energy; the Innovative Molecular Analysis Technology Program of the National Cancer Institute; and the National Science Foundation.

<sup>1</sup>T. Vilker, D. Janasek, and A. Manz, *Anal. Chem.* **76**, 3373 (2004).

<sup>2</sup>D. J. Beebe, G. A. Mensing, and G. L. Walker, *Annu. Rev. Biomed. Eng.* **4**, 261 (2002).

<sup>3</sup>J. Israelachvili, *Intermolecular and Surface Forces*, 2nd ed. (Academic, London, 2003).

<sup>4</sup>D. Stein, M. Kruithof, and C. Dekker, *Phys. Rev. Lett.* **93**, 035901 (2004).

<sup>5</sup>A. Plecis, R. B. Schoch, and R. Philippe, *Nano Lett.* **5**, 1147 (2005).

<sup>6</sup>R. Karnik, R. Fan, M. Yue, D. Li, P. Yang, and A. Majumdar, *Nano Lett.* **5**, 943 (2005).

<sup>7</sup>Q. S. Pu, J. S. Yun, H. Temkin, and S. R. Liu, *Nano Lett.* **4**, 1099 (2004).

<sup>8</sup>R. Karnik, K. Castelino, R. Fan, P. Yang, and A. Majumdar, *Nano Lett.* **5**, 1638 (2005).

<sup>9</sup>R. Fan, Y. Min, R. Karnik, A. Majumdar, and P. Yang, *Phys. Rev. Lett.* **95**, 086607 (2005).

<sup>10</sup>H. Daiguji, P. Yang, and A. Majumdar, *Nano Lett.* **4**, 137 (2004).

<sup>11</sup>C. A. Haynes and W. Norde, *Colloids Surf., B* **2**, 517 (1994).

<sup>12</sup>S. Satyanarayana, R. Karnik, and A. Majumdar, *J. Microelectromech. Syst.* **14**, 392 (2005).

<sup>13</sup>J. W. Donovan and K. D. Ross, *Biochemistry* **12**, 512 (1973).